Influence of a hybrid drying combined with infrared and heat pump dryer on drying characteristics, colour, thermal imaging and bioaccessibility of phenolics and antioxidant capacity of mushroom slices

Senanur Durgut Malçok,[1] Azime Özkan Karabacak,[2,3] Ertürk Bekar,[1,3] Cüneyt Tunçkal,[4] Canan Ece Tamer[1]

[1]Faculty of Agriculture, Department of Food Engineering, Bursa Uludag University, Gorukle, Bursa; [2]Gemlik Asim Kocabiyik Vocational School, Food Technology Program, Bursa Uludag University, Gemlik, Bursa; [3]Science and Technology Application and Research Center, Bursa Uludag University, Gorukle, Bursa; [4]Electric and Energy Department, Air Conditioning and Refrigeration Technology Program, Yalova Community College, Yalova University, Turkey

Abstract

An infrared-assisted heat pump drying (IR-HPD) was designed and used for drying of mushroom slices at three different infrared (IR) powers (50, 100, and 150 W) and a fixed drying temperature of 40°C and air velocity of 1 m/s. The changes in total phenolic content (TPC), total antioxidant capacity (TAC) and individual phenolic contents bioaccessibility, drying characteristics, and colour values of mushroom slices were investigated. IR-HPD provided 13.11 to 30.77% higher energy savings than HPD and reduced drying time between 9.48 and 26.72%. Page, Modified Page models were considered the best for predicting the thin layer drying behaviour of mushroom slices. The effective moisture diffusivity (D_{eff}) value increased with IR power and ranged between $6.491x10^{-10}$ and $9.023x10^{-10}$ m^2s^{-1}. The contents of TPC, TAC, and individual phenolics in mushroom slices were significantly reduced ($p<0.05$) after drying. *In vitro* the bioaccessibility of phenolic compounds and TAC generally decreased, whereas TPC bioaccessibility was increased. Colour values were decreased except for *a** value that increased after drying. Thermal imaging results showed that IR lamps increase the temperature of the products in the middle close to the lamp by approximately 1.5°C. In addition, thermal imaging gave a better understanding and visualised the effect of different power IR lamps on the temperature distribution of the products according to their distance from the lamp. As a result, drying mushrooms with a hybrid drying system combined with IR and heat pump dryer provided higher energy savings than HPD, reduced drying time, and maintained the physical and nutritional characteristics of mushrooms. Overall, the use of IR-HPD is an alternative tool that allows us to obtain high-quality dried mushrooms with good nutritional attributes and a high amount of bioaccessible polyphenols.

Correspondence: Canan Ece Tamer, Bursa Uludag University, Faculty of Agriculture, Department of Food Engineering, 16059, Gorukle, Bursa, Turkey.
E-mail: etamer@uludag.edu.tr

Key words: infrared-assisted heat pump drying (IR-HPD); mushroom; bioaccessibility.

Contributions: the authors contributed equally.

Conflict of interest: the authors declare no potential conflict of interest.

Funding: none.

Received: 6 March 2023.
Accepted: 23 May 2023.

Journal of Agricultural Engineering 2023; LIV:1537
doi:10.4081/jae.2023.1537

Introduction

Cultivated mushroom (*Agaricus bisporus*) is accepted as a high protein, low-calorie food with meditative features. It contains a variety of minerals (K, P, Mg, Ca, Cu, Fe, and Zn), vitamins (vitamin C, B_2, B_3, B_{12}, folate, and D), and dietary fibre (chitin, β-D-glucans, and mannans) and also rich in polyphenols, flavonoids and carotenoids, having an antioxidant activity (Jaworska *et al*., 2015). Due to their exceptional qualities as antioxidants, anti-inflammatory, or antitumor agents, phenolics, one of the bioactive components found in mushrooms, have gained popularity (Palacios *et al*., 2011; Taskin *et al*., 2021). Numerous studies have been conducted on the antioxidant activity, total and individual phenolics of several edible mushrooms in Turkey and other states in the world (Barros *et al*., 2009; Gursoy *et al*., 2009; Nowacka *et al*., 2015; Taskin *et al*. 2021). The phenolic profile of *Agaricus bisporus* revealed only phenolic acids, among which gallic, caffeic, p-hydroxybenzoic, p-coumaric, chlorogenic, trans-cinnamic, protocatechuic and ferulic (Gasecka *et al*., 2018a, 2018b).

Mushrooms are very perishable due to their high water activity, respiration rate, and enzymatic activity, and the shelf life of fresh mushrooms is only about one day in environmental conditions (Mirzaei-Baktash *et al*., 2022). For this reason, mushrooms are traded primarily in processed form in the global market, and dried mushrooms are valuable ingredients in sauces and instant soups as a natural flavouring for culinary purposes.

Several drying methods for mushrooms are reported, including sun drying, vacuum drying (Gopirajah *et al*., 2018), freeze-drying (Piskov *et al*., 2020), conventional hot air drying (Ghanbarian *et al*., 2016), microwave drying (Lombrana *et al*., 2010), vacuum and freeze-drying (Ucar & Karadag, 2019), heat

pump drying (Peter *et al*., 2021; Zhang *et al*., 2022), infrared (IR) drying (Doymaz, 2014) and novel solutions: e.g., solar assisted heat pump dryer (Sevik *et al*., 2013; Xu *et al*., 2021) and pulsed electric field together with ultrasound (Li *et al*., 2021). Preferring the convenient drying method can be the key to a successful operation since mushrooms are very sensitive to temperature (Ghanbarian *et al*., 2016). There are also some limitations to the abovementioned drying methods. For example, sun-drying is unhygienic; vacuum drying is time-consuming due to its low diffusion coefficient; microwave drying causes the burning of mushrooms besides limiting temperature control; and freeze-drying is very high priced (Gopirajah *et al*., 2018). Moreover, according to literature findings, drying methods affect the bioactive components of fruits and vegetables.

Maximising energy savings, efficiency and improving product quality are key points of drying. Heat pump drying (HPD) improves product quality and produces a range of precise conditions. HPD is an eco-friendly technology because it has a closed-controlled system with higher energy efficiency when compared to conventional dryers (Deng *et al*., 2014). Moreover, IR drying is quite suitable, especially for thin product slices depending on its uniform heat distribution, fast drying rate without the risk of burning the material, minimising losses, and simplicity of the equipment (Doymaz, 2014). The structural quality and biological function of the material is improved, and operation costs are decreased. A hybrid drying combining IR and HPD has been utilised as an effective and fast drying method compared to HPD alone. In addition, combining IR with other drying methods preserves the quality of foods, providing uniform heating and better control over temperature (Delfiya *et al*., 2022). In the literature, IR drying and its combination with other technologies such as hot air, vacuum and heat pump were used for drying pears, carrots, and strawberries (Adak *et al*., 2017; Doymaz, 2023, Geng *et al*., 2022; Topuz *et al*., 2022). In this study, the infrared-assisted heat pump drying (IR-HPD) system was first used for mushroom drying.

In engineering, thermal imaging is one of the most frequently used tools to determine temperature distribution. Besides, thermal imaging is an effective method for examining the temperature distribution of products in a non-contact and non-destructive manner (Ali *et al*., 2020). In light of the literature, thermal imaging can be used for temperature verification and showing the temperature distribution in the products during the drying process. IR thermal imaging cameras were used to clearly show the temperature distribution as Cao *et al*. (2017) and Liu *et al*. (2016) evaluated the change in temperature during the microwave drying process. However, until now, no study has been carried out in which food is dried by placing the thermal camera in an IR-HPD. Therefore, in this study, the temperature distribution of the mushroom samples during the drying process was investigated for the first time with thermal imaging. In addition, as far as is known, no study has been found in which the phenolic profile of dried mushrooms has been revealed. Thus, the other originality of this work comes from the quantification of phenolics of IR-HP dried mushrooms using Liquid chromatography tandem-mass spectrometry (LC-MS/MS) method. Moreover, this study attempts to evaluate drying kinetics and several quality attributes (colour, thermal imaging, bioaccessibility of total and individual phenolics and antioxidant capacity) of mushroom slices dried by IR-HPD. The design engineers, vegetable suppliers, and nutritionists will also profit from this extensive research.

Materials and Methods

Materials

Fresh mushrooms (*Agaricus bisporus*) were purchased from a local market in Yalova, Turkey. Mushrooms were washed with tap water, wiped and sliced (6 mm thick) using a steel cutter, and immediately dried. The initial moisture content of the mushrooms was measured as 7.459±0.01 g water/g dry weight (dw) using an oven (Shimadzu-MOC63u) at 105±3°C.

Hybrid drying system procedure

IR-HPD (Figure 1), designed at Yalova University, Turkey, was used for hybrid drying. The HPD system is a closed-loop conduit system without outside air intake during drying. The system consists of two parts: the refrigerant and drying air cycles. In the refrigerant process, the system consists of four main elements. (1-2) The compressor where the compression work is carried out and the gas pressure and temperature are increased, (2-3) the condenser where the gas pressure is held constant, and the temperature is reduced, (3-4) the capillary tube where the gas pressure is reduced, and finally (4-1) evaporator (between 1 and 5°C) where the liquid refrigerant boils with reduced pressure. The thermostat controls the drying temperature in the system. When the thermostat reaches the desired drying temperature, it allows gas to pass through the external condenser (3') with the help of solenoid valves. The gas flow to the external condenser stops when the drying temperature falls below the desired value. This process occurs automatically, and the system operates in the differential range of 1°C. In the air side process, there is a continuous air flow without an outside air inlet, thanks to an axial fan. An internal condenser and evaporator are in the air duct. At point (A), the air heated by the internal condenser enters the drying cabinet leaving the drying cabinet at point (B) with moisture from the product. After point (C) passes through the evaporator inlet, it condenses at point (D) thanks to the evaporator and leaves its moisture. The drying air cools as it passes through the evaporator. It comes to the internal condenser (E) to increase its temperature again. This process continues during drying. Thanks to the data logger (j) seen in Figure 1 from the points specified in the air process, temperature and relative humidity (changed during drying between 12% and 20%) are measured at one-minute intervals. In the HPD system, only the heat of the gas in the condenser is used as the heat source. This causes the compressor to be forced and consume more energy. For IR-HPD drying, an IR lamp was placed in the drying cabinet of the system to assist the heat source. The weight loss of the product was recorded at three-minute intervals thanks to the load-cell (k). The energy consumed by the whole system and the compressor during drying was measured and recorded via the energy meters placed on the system.

Four different drying conditions were tested; i) HPD without IR power (control); ii) HPD with IR power at 50 W; iii) HPD with IR power at 100 W; iv) HPD with IR power at 150 W. HPD was conducted under the temperature of 40°C and air velocity of 1 m/s. Our previous research chose this air velocity as optimum value (Tunckal *et al*., 2022). In all cases, 425±5 g fresh mushroom slices were placed in the dryer as a single layer. All of the drying experiments were performed three times down to a final moisture content of 0.135±0.01 g water/g dw (Ucar & Karadag, 2019).

Mathematical modelling of drying kinetics

Seven thin layer drying models used for describing IR-HPD drying data of mushrooms were given as following equations

(Coşkun *et al*., 2017):

Page MR = exp(-kt ^{n}) (1)

Modified page MR= exp [(-kt) ^{n}] (2)

Logarithmic MR = a exp(-kt) + c (3)

Lewis MR = exp(-kt) (4)

Henderson and Pabis MR = a exp(-kt) (5)

Two Term Exponential MR=a exp(-kt)+(1-a) exp(-kat) (6)

Wang and Singh MR=1+at+bt^2 (7)

In the modelling, the following equation (8) was used to calculate moisture ratio (MR) on a dry basis.

$$MR = \frac{M - M_e}{M_i - M_e} \quad (8)$$

where M represents the moisture content at a specific time (g water/g dw), M_i is the moisture content of the sample prior to drying (g water/g dw), and M_e is the equilibrium moisture content (g water/g dw).

$$Drying\ rate = \frac{M_{t+dt} - M_t}{dt} \quad (9)$$

In this formula, t is drying time (min), M_t is the moisture content at the time of t and M_{t+dt} is the moisture content at the time of $t+dt$ (g water/g dry base).

The greater the value of R^2, the less the values of Chi-square (χ^2) and root mean square error (RMSE) indicate the better model for mathematical approximation of drying curves. These values were given in the following equation (10) and (11).

$$RMSE = \left[\frac{1}{N}\sum_{i=1}^{N}(MR_{exp,i} - MR_{pre,i})^2\right]^{1/2} \quad (10)$$

$$\chi^2 = \frac{\sum_{i=1}^{N}(MR_{exp,i} - MR_{pre,i})^2}{N - n} \quad (11)$$

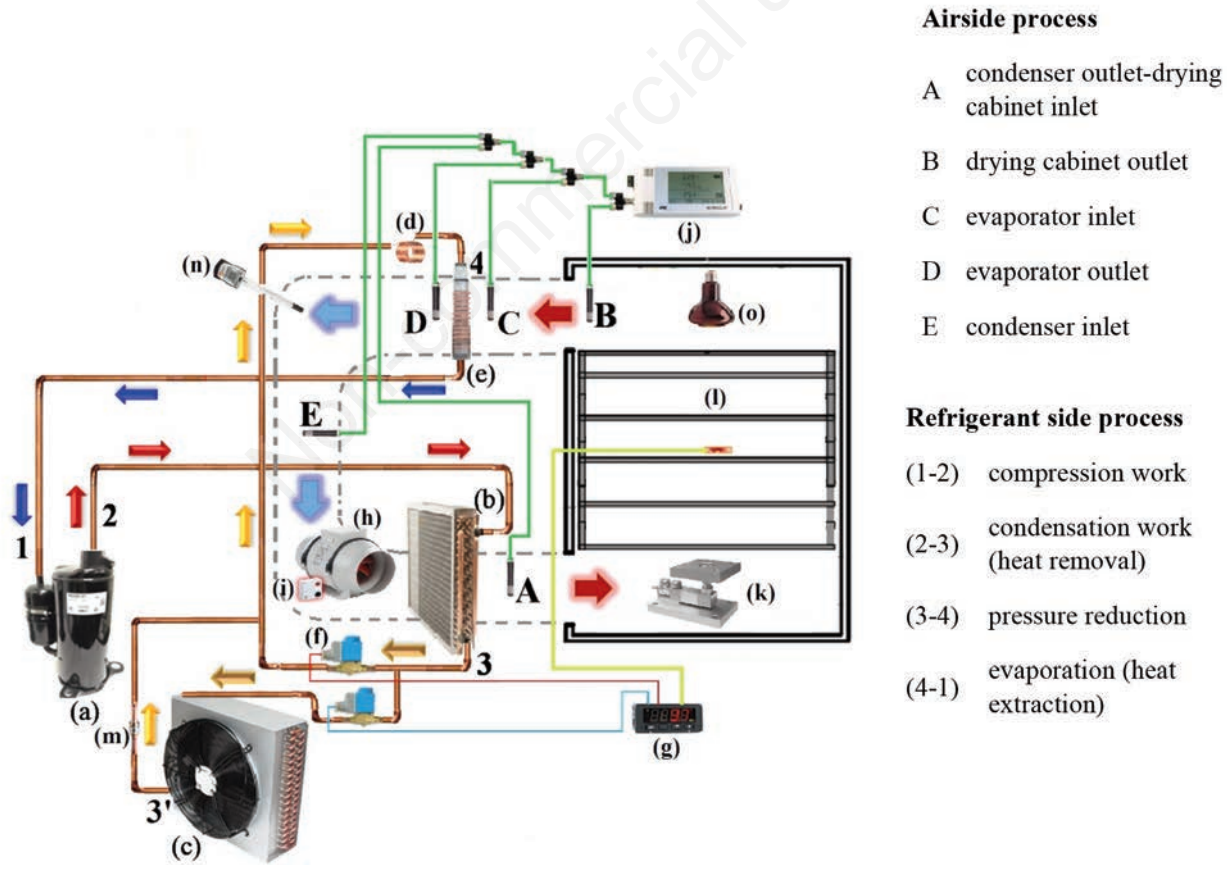

Figure 1. Experimental set-up. **a**) compressor; **b**) internal condenser; **c**) external condenser; **d**) capillary tube; **e**) evaporator; **f**) solenoid valve; **g**) thermostat; **h**) axial fan; **i**) speed switch; **j**) data logger; **k**) load-cell; **l**) drying cabined; **m**) check valve; **n**) anemometer; **o**) infrared lamp. Refrigerant side process: (1-2) compression work; (2-3) condensation work (heat removal); (3-4) pressure reduction; (4-1) evaporation (heat extraction). Airside process: A) condenser outlet-drying cabinet inlet; B) drying cabinet outlet; C) evaporator inlet; D) evaporator outlet; E) condenser inlet.

In these equations, $MR_{exp,i}$ is the experimental moisture ratio of the i^{th} test and $MR_{pre,i}$ is the dimensionless moisture ratio of the i^{th} *test*. *N* represents observation numbers, and *n* is the number of model constants.

Effective moisture diffusivity

Fick's second law in diffusion with infinite slab geometry was used to calculate the effective moisture diffusivity. According to the assumptions in the drying process of mushroom slices with a uniform initial moisture distribution throughout the mass of a sample, constant effective diffusivity coefficient, symmetric mass transfer towards to the centre, negligible resistance to the mass transfer at the surface, considering mass transfer only by diffusion and negligible shrinkage during drying, the effective moisture diffusion equation for infinite slab geometry is presented in the equation (12) (Crank, 1975):

$$MR = \frac{8}{\pi^2}\sum_{n=1}^{\infty}\frac{1}{(2n-1)^2}\exp\left(-\frac{(2n-1)^2\pi^2 D_{eff}t}{4L^2}\right) \quad (12)$$

where D_{eff}, L and n are effective moisture diffusivity (m^2/s), the characteristic dimension of half thickness (m), respectively. The equation is simplified to the straight-line equation as equation (13):

$$D_{eff} = -\frac{slope 4L^2}{\pi^2} \quad (13)$$

Analysis methods

Determination of total phenolic content and total antioxidant capacity

Firstly, undigested parts of mushroom slices were extracted using the method described by Kamiloglu and Capanoglu (2014). Until analysis, extracts were stored at -20°C.

Total antioxidant capacity (TAC) and total phenolic content (TPC) of mushroom samples were measured using an ultraviolet-visible spectrophotometer (UV-1800, Shimadzu). The Folin-Ciocalteu method described by Velioglu *et al*. (1998) was used for determining the TPC of mushroom samples. The results were expressed in terms of mg gallic acid equivalent (GAE)/100 g dw. The TAC of samples was analysed using 2,2-Diphenyl-1-picrylhydrazyl (DPPH) and ferric reducing antioxidant power (FRAP) methods according to Kumaran and Joel Karunakaran (2006) and Benzie and Strain (1996), respectively. The TAC results were expressed as µmol trolox equivalent (TE)/g dw (R^2=0.9992).

Phenolic composition

LC-MS/MS analysis of individual phenolic compounds carried out using Shimadzu LC-MS/MS 8060 system (Shimadzu Corporation, Kyoto, Japan) equipped with C18 analytical column (3 µm particle size, 200 Å pore size, 100 mm × 3 mm, High Purity ES Silica Gel LC Column; GL Sciences, Tokyo, Japan). Electrospray ionisation source was used for operating the MS/MS system in negative and positive ion modes with multiple reaction monitoring. LabSolution (Shimadzu Corporation, Kyoto, Japan) software was used for data monitoring.

Instrument settings were as follows: nebulising gas (N_2) flow 3.0 L/min, drying gas (N_2) flow 10.0 L/min, interface voltage 4.0 kV, desolvation line temperature 250°C, interface temperature 300°C, heat block temperature 400°C. The LC-MS/MS method was carried out by modifying the study of (Vu *et al*., 2018). The run time for each injection (10 µL) was 15 min, and the column oven temperature was 40°C. The elution gradient (Table 1) was created from mobile phase A (MQ water with 0.1% formic acid) and mobile phase B (acetonitrile with 0.1% formic acid) within 0.4 mL/min total flow.

In vitro gastrointestinal digestion

In vitro, gastrointestinal digestion of the mushroom samples was prepared using the method of (Minekus *et al*., 2014), with some modifications. Gastric and intestinal digestions of samples were simulated. Simulated gastric fluid, porcine pepsin solution (25.000 U/mL, Sigma-Aldrich P6887; USA), and calcium chloride were mixed during the gastric phase. The pH of this solution was then adjusted to 3 by using hydrochloric acid. After, the mixture was incubated at 37°C for 2 hours in a shaking water bath (Memmert SV 1422, Memmert GmbH & Co., Germany). 4 mL aliquots were obtained for each test tube. The residue of the gastric phase was mixed with the simulated intestinal fluid, pancreatin solution (800 U/mL, Sigma Aldrich P3292) and bile solution (160 mM). The pH was adjusted to 7.0 with sodium hydroxide. In a shaking water bath, the intestinal phase was incubated at 37°C for 2 hours. Finally, the mixture was centrifuged at 3500 rpm for 10 min, filtered, and the supernatant was obtained. Until analysed, the simulations after gastric digested phases and after intestinal digested phases were kept at -20°C.

Colour analysis

Colour parameters of mushroom slices were evaluated using a CR-5 Konica Minolta Chroma Meter (Osaka, Japan). This analysis was performed in triplicate, and *L*, a*, b*, C*, and h°* values were determined. Colour values were expressed as *L** (lightness/darkness), *a** (greenness/redness) and *b** (blueness/yellowness). In addition, *C** and *h°* (hue angle) symbolise colour intensity and an angle between 0° and 360°, respectively. ΔE^*_{ab} indicates the total colour change after drying, which was determined using the following equation:

$$\Delta E^*_{ab} = \sqrt{(L^* - L^*_0)^2 + (a^* - a^*_0)^2 + (b^* - b^*_0)^2} \quad (14)$$

where, L_0*, a_0* and b_0*, and are the colour values of fresh mushroom slices.

Infrared lamps and thermal imaging

In this study, IR lamps with different powers (50, 100, 150 W) were placed in the middle of the ceiling of the cabinet. The effects of IR lamps on the temperature distribution of the cabinet and products were evaluated by thermal imaging processes. Fluke Ti9

Table 1. Elution gradient conditions.

Line A, %	Line B, %	Time (min)
80-80	20-20	0.00-0.50
80-50	20-50	0.50-7.00
50-5	50-95	7.00-12.00
5-80	95-20	12.00-12.10
80-80	20-20	10.00-15.00

thermal camera was used for this process. The images of the cabinet and the trays containing the products were taken from 1 m and 0.5 m distances, respectively.

Statistical analysis

Statistical analysis was performed using the IBM SPSS Statistics 23 software (IBM SPSS, USA). The analysis of variance (ANOVA) and Duncan's multiple range test were conducted to determine significant differences between means at the 5% significance level. Each measurement was conducted in triplicate, and the results were expressed as mean ± standard deviation.

Results and Discussion

Drying kinetics of mushroom slices

The drying time versus moisture content of dried mushroom slices is given in Figure 2. Mushroom slices with an initial moisture content of 7.459±0.01 g water/ g dw were dried by IR-HPD at 40°C with 50, 100, and 150 W IR powers until their final moisture was 0.135±0.01 g water/ g dw. The drying times for the control sample and the different IR power (50 W, 100 W and 150 W) applied samples were found to be 348, 315, 288, and 255 min., respectively. It was seen that the drying time was the longest in the control sample without IR. Applying IR shortened the drying time between 33 and 93 min, resulting in time saving between 9.48 and 26.72%. The results showed that drying took shorter as IR power increased. In the study of (Khampakool *et al*., 2019), the drying time of IR-assisted freeze-dried banana snacks was 70% less when compared to freeze-drying. Another study showed that the IR-assisted hot air drying method accelerated the drying time by 23% compared to hot air drying (Abbaspour-Gilandeh *et al*., 2020). Moreover, when comparing water blanched – hot air-dried carrot slices, the reduction of drying time was 45% in IR-blanched and IR-assisted hot air-dried samples (Vishwanathan *et al*., 2013). The reduced drying time in the combined mode of IR with other drying methods might be caused by the fact that the synergistic effect heats the foods quicker because of high heat and mass transfer rates (Delfiya *et al*., 2022). IR-HPD not only shortened the drying time but also gave advantageous results regarding total energy consumption. The total energy consumption of the system for the control sample and the samples dried in IR-HPD (50 W, 100 W, and 150 W) was found to be 3.897, 3.386, 3.076, and 2.698 kWh, respectively. Using IR for assisting HPD provided 13.11 to 30.77% less energy consumption than the control sample. The results indicated that total energy consumption decreased by increasing IR power as an assisting heat source. The same trend was obtained using IR as assisted convective hot air drying, vacuum drying, innovative interval IR airflow drying, freeze-drying, and HPD.

The variations in the drying rate against the moisture content of dried mushroom slices are shown in Figure 3. The highest drying rate was obtained at 150 W, followed by 100 W, 50 W, and the control sample without IR. Applying IR for HPD increased the drying rate between 9.94 and 59.94%. The increment in drying rate by increasing IR power was observed since more energy application resulted in rapid heating of the material and faster water removal (Delfiya *et al*., 2022). A similar increase in drying rate with an increase in IR power was reported for longan fruit, jujube, sour cherry, potato, apricot pomace, corn, and grated carrot.

The drying rate was higher at the beginning of drying when the moisture content was the highest, maybe because the free moisture near the surface of the mushroom slices was removed early in the process and then reduced with reducing moisture content. Although all drying conditions generally occurred in the falling rate period, accelerated drying rates were sometimes observed due to internal heat generation. Moreover, it can be seen in Figure 3 that there was not a constant rate period due to the thin layers of the mushroom slice that did not ensure a constant supply of water during dehydration. Other studies such as Sadeghi *et al.* (2020) reported the falling rate period without constant rate during drying.

Modelling of drying data

When mathematical models are used to describe the drying characteristics of foods, it is easy to monitor process management and instrument functioning (Sufer & Palazoglu, 2019). After determining the MR of the drying treatments and fitting the model with the experimental data, R^2, χ^2, and RMSE were obtained for each model (Table 2). R^2 of all models for all drying treatments varied in the range of 0.8825-0.9956, while their χ^2 and RMSE ranged from 0.000181 to 0.057493 and 0.001350 to 0.021977, respectively. In all drying conditions, Page and Modified Page models had a higher value of R^2 but a lower value of RMSE and χ^2 when compared with other applied models. Therefore, Page, Modified Page models were considered to be the best for predicting the thin layer drying behaviour of mushroom slices. Similar findings were reported by Khampakool *et al*. (2019) for IR-assisted freeze drying of bananas and Kantrong *et al*. (2014) for microwave-vacuum combined with IR drying of mushrooms.

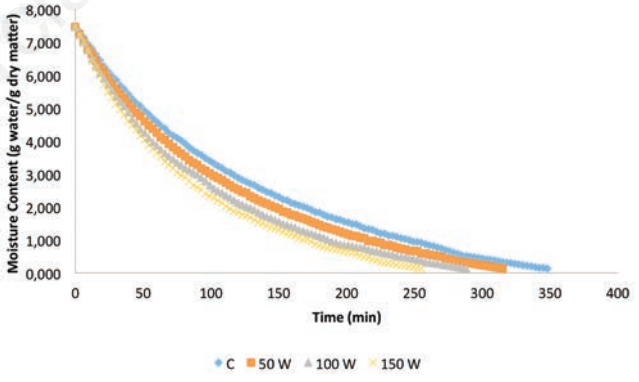

Figure 2. The drying time versus moisture content of mushroom slices dried by infrared-assisted heat pump drying.

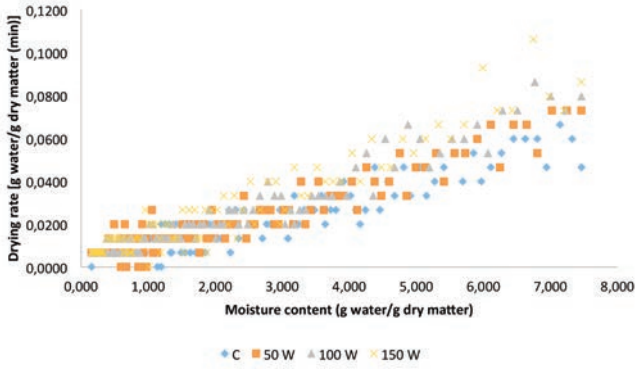

Figure 3. Drying rates of mushroom slices dried by infrared-assisted heat pump drying.

Effective moisture diffusivity (D_{eff})

D_{eff} is a standard mass transfer parameter that considers molecule, liquid, and vapour diffusion and other potential mass transport mechanisms (Das *et al*., 2009). D_{eff} values of mushroom slices during HPD and IR-HPD were presented in Figure 4. D_{eff} values were changed between $6.491´10^{-10}$ and $9.023´10^{-10}$ m^2s^{-1}, which was in the range of mostly reported values for biological materials (10^{-12} to 10^{-8} m^2s^{-1}). As the literature demonstrates, the drying technique and condition are just as important in controlling moisture diffusion inside biological products as their inherent features (Geng *et al*., 2022). In the IR-assisted samples, the D_{eff} value increased up to 39% compared to the control. The results indicated a direct relationship between D_{eff} and the IR power (Figure 4). The increment in IR power resulted in an increase in D_{eff} since the faster rise in food temperature increased the vapour pressure and caused rapid moisture diffusion to the surface (Shi *et al*., 2008). This phenomenon may be explained by the molecular vibration, rotation, and electronic states of the atom increased by higher intensity that

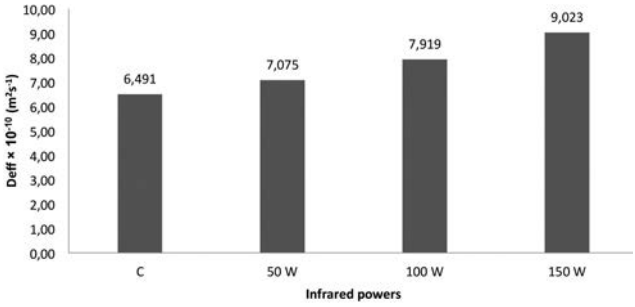

Figure 4. Effect of heat pump drying and infrared-assisted heat pump drying on Deff values of dried mushroom slices. C, control sample dried at 40°C with heat pump drying; 50 W, dried at 40°C with 50 W infrared-assisted heat pump drying; 100 W, dried at 40°C with 100 W infrared-assisted heat pump drying; 150 W, dried at 40°C with 150 W infrared-assisted heat pump drying.

Table 2. Statistical results obtained from the modelling of mushroom slices.

Models			C	50 W	100 W	150 W
Page	Model coefficient	n	1.0588	1.0174	1.0171	1.0303
		k	0.0063	0.0088	0.0102	0.0107
	R^2		0.9926	0.9934	0.9956	0.9948
	RMSE		0.001705	0.001537	0.001350	0.001499
	χ^2		0.000346	0.000255	0.000181	0.000198
Modified Page	Model coefficient	n	1.0588	1.0174	1.0171	1.0303
		k	0.0083	0.0096	0.0110	0.0122
	R^2		0.9926	0.9934	0.9956	0.9948
	RMSE		0.001705	0.001537	0.001350	0.001499
	χ^2		0.000346	0.000255	0.000181	0.000198
Logarithmic	Model coefficient	k	0.0121	0.0130	0.0146	0.0168
		a	1.4608	1.3660	1.3378	1.3789
		c	0.0181	0.0181	0.0179	0.0169
	R^2		0.8825	0.9037	0.9181	0.9078
	RMSE		0.011839	0.010237	0.009813	0.011522
	χ^2		0.016832	0.011432	0.009639	0.011831
Lewis	Model coefficient	k	0.0080	0.0102	0.0115	0.0130
	R^2		0.9500	0.9617	0.9738	0.9673
	RMSE		0.001618	0.002767	0.002233	0.002668
	χ^2		0.000309	0.000819	0.000489	0.000619
Henderson and Pabis	Model coefficient	k	0.0100	0.0109	0.0122	0.0139
		a	1.2353	1.1803	1.1459	1.1689
	R^2		0.9605	0.9684	0.9782	0.9729
	RMSE		0.006200	0.005259	0.004471	0.005361
	χ^2		0.004575	0.002988	0.001980	0.002530
Two term exponential	Model coefficient	k	0.0064	0.0071	0.0080	0.0090
		a	0.5526	0.5414	0.5340	0.5389
	R^2		0.9605	0.9684	0.9782	0.9729
	RMSE		0.014107	0.016309	0.017903	0.018331
	χ^2		0.023689	0.028738	0.031744	0.029586
Wang and Singh	Model coefficient	b	0.00001	0.00002	0.00002	0.00003
		a	-0.0070	-0.0083	-0.0095	-0.0104
	R^2		0.9398	0.9196	0.9255	0.9363
	RMSE		0.021977	0.010495	0.014891	0.009238
	χ^2		0.057493	0.011901	0.021963	0.007515

C, control sample dried at 40°C with HPD; 50 W, dried at 40°C with 50 W IR-HPD; 100 W, dried at 40°C with 100 W IR-HPD; 150 W, dried at 40°C with 150 W IR-HPD; RMSE, root mean square error.

causes enhanced temperature and vapour pressure of food materials; thus, the moisture diffusion to the surface of the sample increased (Delfiya *et al*., 2022). This explanation was compatible with Das *et al*. (2009)'s study in which the drying properties of high moisture paddy were investigated for five levels of radiation intensity (1509, 2520, 3510, 4520, and 5514 W/m^2) and four levels of grain bed depths under various vibrating settings. Moreover, the same trend in our study was observed by Doymaz (2023). He investigated different IR powers (50, 62, 74, and 88 W) on some quality parameters of pear slices. In the literature, during IR and IR-assisted drying of food materials, D_{eff} values were changed between 10^{-11} and 10^{-7} m^{2}s^{-1}. Among these findings, the highest D_{eff} value of 1.056×10^{-7} to 1.7989×10^{-7} was obtained by drying shrimp with hybrid IR-hot air convection (Tirawanichakul *et al*., 2008).

An increase in D_{eff} values with an increase in IR power has been reported in drying kiwifruit, potato, sour cherry, pumpkin slices, and button mushrooms.

Effect of hybrid drying on total phenolic content and total antioxidant capacity values and their bioaccessibility in mushroom slices

TPC values of undigested, *in vitro* simulated gastric digested, and *in vitro* simulated intestinal digested mushroom samples were shown in Table 3. TPC of undigested samples was determined between 126.75 and 233.93 mg GAE/100 g. The highest TPC value was found in fresh mushroom samples. Zeng *et al*. (2012) investigated 5 different Australian edible mushrooms, and determined the TPC of mushrooms using the Folin-Ciocalteu method. According to this research, the TPC of samples was measured between 63.4 and 282.3 mg GAE/100 g DM. Results showed that the TPC of different mushroom samples may change depending on different geographical locations. In addition, harvest conditions affect the characteristic composition of mushrooms. When all samples were compared in our study, fresh mushroom samples had the highest phenolic content after *in vitro* intestinal digestion. When the IR power increased from 50 W to 100 W, the TPC values of *in*

Table 3. Total phenolic content of mushroom slices before and after *in vitro* simulated gastric and intestinal digestion.

Sample	Undigested (mg GAE/100 g dw)	Simulated gastric digestion (mg GAE/100 g dw)	Simulated intestinal digestion (mg GAE/100 g dw)
F	233.93±2.48^{aC}	388.60±1.19^{bB}	666.79±3.07^{aA}
C	180.76±8.77^{bB}	276.58±7.84^{cA}	285.06±1.28^{eA}
50 W	183.43±8.58^{bB}	128.38±6.89^{eC}	410.91±1.09^{cA}
100 W	165.16±9.04^{bC}	424.63±2.17^{aB}	567.82±2.05^{bA}
150 W	126.75± 9.82^{cC}	245.76±8.77^{dB}	361.94±1.49^{dA}

F, sample of fresh mushroom; C, control sample dried at 40°C with HPD; 50 W, dried at 40°C with 50 W IR-HPD; 100 W, dried at 40°C with 100 W IR-HPD; 150 W, dried at 40°C with 150 W IR-HPD; GAE, gallic acid equivalent. ^{a,b}Values followed by different lower letters within the same column are significantly different ($p<0.05$); ^{A,B}values followed by different capital letters within the same row are significantly different ($p<0.05$).

Table 4. Total antioxidant capacity (2,2-Diphenyl-1-picrylhydrazyl) of mushroom slices before and *in vitro* simulated gastric and intestinal digestion.

Sample	Undigested (µmol TE/g dw)	Simulated gastric digestion (µmol TE/g dw)	Simulated intestinal digestion digestion (µmol TE/g dw)
F	46.18±1.19^{aA}	50.75±0.51^{bA}	35.83±3.20^{bA}
C	44.28±1.51^{aA}	34.22±1.29b^{AB}	26.72±1.63^{bB}
50 W	49.12±1.65^{aA}	28.49±0.96^{bB}	43.45±1.59^{bA}
100 W	39.44±1.05^{aB}	85.53±0.21^{aA}	68.64±1.30^{aAB}
150 W	24.32±2.27^{bB}	37.07±0.60b^{AB}	41.52±1.10b^{A}

F, sample of fresh mushroom; C, control sample dried at 40°C with HPD; 50 W, dried at 40°C with 50 W IR-HPD; 100 W, dried at 40°C with 100 W IR-HPD; 150 W, dried at 40°C with 150 W IR-HPD; TE, trolox equivalent. ^{a,b}Values followed by different lower letters within the same column are significantly different ($p<0.05$); ^{A,B}values followed by different capital letters within the same row are significantly different ($p<0.05$).

Table 5. Total antioxidant capacity (ferric reducing antioxidant power) of mushroom slices before and in vitro simulated gastric and intestinal digestion.

Sample	Undigested (µmol TE/g dw)	Simulated gastric digestion (µmol TE/g dw)	Simulated intestinal digestion digestion (µmol TE/g dw)
F	32.79±0.42^{aA}	25.52±2.81^{bB}	14.32±1.03^{dC}
C	32.55±1.75^{aA}	19.73±1.84^{cC}	28.54±2.31^{bB}
50 W	29.57±2.84^{abA}	18.09±1.72^{cC}	23.01±1.93^{cB}
100 W	26.02±4.76^{bC}	44.38±2.08^{aA}	33.49±0.55^{aB}
150 W	14.53±1.43^{cB}	16.74±1.16^{cA}	14.28±0.35^{dB}

F, sample of fresh mushroom; C, control sample dried at 40°C with HPD; 50 W, dried at 40°C with 50 W IR-HPD; 100 W, dried at 40°C with 100 W IR-HPD; 150 W, dried at 40°C with 150 W IR-HPD; TE, trolox equivalent. ^{a,b}Values followed by different lower letters within the same column are significantly different ($p<0.05$); ^{A,B}values followed by different capital letters within the same row are significantly different ($p<0.05$).

vitro simulated gastric and intestinal digested samples were increased (Table 3). Kayacan *et al*. (2020) investigated the effect of different drying methods on the biochemical properties of persimmons. They reported that the release of bounded phenolic components by heat treatment during the drying procedure leads to increasing bioaccessibility of TPC and TAC. This situation was valid for undigested and digested samples except for the simulated *in vitro* gastric digested sample that was dried by IR-HPD at 50 W (Table 3). However, when mushroom slices dried at 150 W IR-HPD, the TPC of all samples decreased. The drying process at more severe conditions may lead to an increase in phenolic compound degradation. Since polyphenols are heat labile and prolonged heat exposure can result in irreversible chemical changes in phenolic compounds, the TPC losses in mushroom slices after drying may be explained. Additionally, further factors like the activity of oxidative enzymes (polyphenol oxidase, peroxidase), the content of organic acids, the concentration of sugar, and the pH can also cause TPC to degrade (Zhou *et al*., 2016). Zhou *et al*. (2017) similarly reported a decrease in TPC when garlic slices were dried by IR at temperatures from 50°C to 80°C and powers from 675 to 2.025 W. The increment of TPC values between undigested and after *in vitro* simulated gastric digested samples ranged between 53 and 157%, except the sample dried at 50 W IR-HPD, in which a 30% decrement was detected. After simulated *in vitro* intestinal digestion, samples had higher TPC values than undigested ones. There was no significant difference in the TPC value of the control (C) sample after *in vitro* simulated gastric digestion and *in vitro* simulated intestinal digestion ($p>0.05$). TPC values increased between 57 and 185% after *in vitro* simulated intestinal digestion compared to undigested samples.

TAC values measured using DPPH and FRAP methods were shown in Tables 4 and 5, respectively. When the two methods were compared, the highest TAC values were obtained in the FRAP method. DPPH values of undigested, *in vitro* simulated gastric digested, and *in vitro* simulated intestinal digested mushroom samples were determined between 24.32-49.12, 28.49-85.53 and 26.72-68.64 µmol TE/g DM, respectively. Islam *et al*. (2016) evaluated TAC of different mushroom samples in China. They determined DPPH values between 1.36 and 18.56 µmol TE/g DM. Leiva-Portilla *et al*. (2020) investigated the effect of two different drying methods on the DPPH values of *Cyttaria espinosae* mushroom samples. The highest TAC was obtained in freeze-dried samples (12.82 µmol TE/g DM). DPPH values of fresh and hot air-dried samples were determined as 9.49 µmol TE/g DM and 8.13 µmol TE/g DM, respectively. Our DPPH results are higher than these results. According to the literature, different mushroom varieties have different TAC. Different species of mushrooms have been reported to include polysaccharides, triterpenes, sterols, lectins and proteins. These components are found in different proportions in each mushroom variety, leading to each mushroom having different biochemical structures. Adak *et al*. (2017) used a convective-IR system for drying strawberries. They chose infrared power from 100 W to 300 W, temperature from 60 to 80°C and velocity from 1.0 m/s and 2.0 m/s. When they increased IR power from 100 W to 300 W, TAC was increased. When air temperature and velocity were 80°C and 2 m/s, the DPPH value was determined for 100 W as 2.88 g/g and 300 W as 5.81 g/g. In our study, when IR power increased from 50 W to 100 W, DPPH and FRAP values of *in vitro* gastric and *in vitro* simulated intestinal digested samples were also increased (Table 4 and Table 5). However, increasing IR power to 150 W led to decrease TAC values of undigested, *in vitro* simulated gastric and intestinal digested samples. The highest DPPH value was obtained from *in vitro* simulated gastric digested sample of 100 W. When the DPPH value of undigested and *in vitro* simulated gastric digested sample dried by IR-HPD at 100 W was compared, the increment of AC was 116%. However, after simulated intestinal digestion, the DPPH value of the sample dried at 100 W IR-HPD decreased 24% compared to *in vitro* simulated gastric digestion.

FRAP values of the samples before digestion, after *in vitro* gastric and after *in vitro* intestinal digestion were measured between 14.53-32.79, 16.74-44.38, and 14.28-33.49 µmol TE/g DM, respectively (Table 5). Naknaen *et al*. (2015) evaluated FRAP values of dried four different edible mushroom samples using by hot air-drying method. They determined between 8.51 and 74.99 µmol TE/g DM. Mushrooms have phenolic acid, monophenolic acid and polyphenolic constituents. These phenolic compounds are effective in the TAC of foods (Zeng *et al*., 2012). In our study, the fresh sample had the highest FRAP value; also, the most phenolic content was detected in fresh mushrooms compared to other samples. Both *in vitro* simulated gastric and intestinal digested samples of fresh, control and IR-HPD (50 W) dried mushroom samples showed lower FRAP values than their undigested ones. The most variation was found in fresh sample (F), showing a 43% decrease between undigested and *in vitro* simulated intestinal digested samples. However, FRAP values of the *in vitro* simulated gastric and intestinal digested samples IR-HPD dried at 100 W had higher than undigested sample. It may be explained by that new phenolic compounds may comprise after digestion. Also, after digestion, some phenolic compounds are released. These formed compounds can contribute to increase in TPC and TAC of foods. TAC of new phenolic compounds formed after *in vitro* gastric and *in vitro* intestinal digestion and released phenolics may not be as high as TAC of phenolic compounds obtained before digestion. This phenomenon may cause to decrease or not to change in TAC when increasing TPC (Rodriguez-Roque *et al*., 2013).

Effect of infrared-assisted heat pump drying on individual phenolic contents and their bioaccessibility in mushroom slices

The effect of HPD and IR-HPD on the phenolic composition of the mushroom slices is shown in Table 6. The analytical parameters are described in Table 7. Totally 13 phenolic compounds, namely; chrysophanol, 3,4-dihydroxybenzoic acid (protocatechuic acid), caffeic acid, 2-hydroxybenzoic acid (*o*-salicylic acid), 4-hydroxybenzoic acid (*p*-salicylic acid), ellagic acid, rutin, hesperidin, quercetin-3-*O*-glucoside (isoquercitrin), vanillin, 4-hydroxycinnamic acid (*p*-coumaric acid), luteolin and quercetin were identified, and their amounts were quantified in the fresh and dried mushroom slices as a result of the LC-MS/MS analysis. Ellagic acid was not detected in undigested samples. Figure 5 shows the LC-MS/MS chromatogram of standard phenolic compounds. The result indicated that the major compound of undigested fresh and dried mushroom extracts was *p*-salicylic acid (9622.43 µg/L dw) (Table 6). Among the phenolic acids, vanillic acid (6.1 µg/g dw) and gallic acid (62.76 µg/g dw) were determined as major phenolic acids in mushroom spices of *Hyphodontia paradoxa* and *Agaricus bisporus*, respectively (Nowacka *et al*., 2015).

The amounts of ellagic acid in both undigested and digested samples remained below the limit of quantification value except the control sample (47.98 µg/kg) after the intestinal phase. Ellagic acid was detected in several mushroom species (*i.e.*, *Morchella esculenta, Clitocybe odora, Laetiporus sulphureus, Leucoagaricus leucothites, Leucopaxillus tricolor, Pleurotus ostreatus, Russula aurora, Russula azurea, Suillus granulatus*) by previous studies

Table 6. Phenolic composition of the fresh and dried mushroom slices (µg/kg dw).

Sample	Chrysophanol	Protocatechuic acid (3,4DHBA)	Caffeic acid	*o*-Salicylic acid	*p*-Salicylic acid (4HBA)	Ellagic acid	Rutin	Hesperidin	Isoquercitrin	Vanillin	*p*-Coumaric acid	Luteolin	Quercetin
Undigested													
F	17.96±0.97^{a}	378.89±18.46^{b}	1860.56±21.87^{a}	3637.66±32.66^{a}	9622.43±573.20^{a}	nd	17.40±1.78^{a}	464.99±7.25^{a}	64.94±2.90^{a}	1563.00±25.62^{a}	2459.91±66.34^{a}	5.60±0.27^{a}	40.00±1.04^{a}
C	2.44±0.19^{b}	149.24±1.41^{d}	135.96±2.58^{d}	795.81±14.56^{c}	7303.99±79.23^{b}	nd	1.66±0.09^{bc}	30.71±1.12^{d}	8.19±0.27^{b}	1277.77±24.29^{b}	65.32±3.74^{c}	1.04±0.05^{c}	6.08±0.06^{b}
50 W	3.13±0.44^{b}	313.06±0.98^{c}	367.73±8.91^{c}	329.88±4.71^{e}	5050.26±250.92^{c}	nd	0.81±0.04^{c}	11.11±0.54^{e}	Nd	354.19±9.16^{c}	43.74±1.45^{cd}	0.47±0.03^{d}	nd
100 W	2.51±0.38^{b}	497.48±13.11^{a}	524.85±11.42^{b}	594.20±7.96^{d}	10182.72±561.25^{a}	nd	2.57±0.16^{b}	104.87±2.48^{b}	8.48±0.06^{b}	272.54±18.48^{e}	358.32±25.27^{b}	2.69±0.06^{b}	4.29±0.11^{c}
150 W	2.73±0.24^{b}	51.28±2.61^{e}	34.81±0.59^{e}	907.29±15.19^{b}	2787.05±69.64^{d}	nd	1.47±0.13^{bc}	81.55±0.45^{e}	3.60±0.06^{c}	312.09±5.31^{d}	nd	1.11±0.17^{c}	1.07±0.02^{d}
Simulated gastric digested													
F	nd	35.51±1.41	nd	1430.74±46.83^{a}	2543.57±34.92^{a}	nd	nd	nd	nd	3983.55±10.87a	nd	nd	nd
C	nd	nd	nd	128.01±5.44^{b}	2108.52±53.41^{b}	nd	nd	4.30±0.23c	nd	568.10±23.58^{b}	nd	nd	nd
50 W	nd	nd	nd	68.14±3.05^{c}	470.73±34.74^{c}	nd	nd	1.98±0.10d	nd	182.50±33.01^{c}	nd	nd	nd
100 W	nd	nd	nd	113.59±3.98^{b}	549.95±29.47^{c}	nd	0.81±0.12^{b}	4.53±0.22^{b}	2.74±0.11^{b}	146.36±21.47^{c}	nd	nd	0.23±0.01^{a}
150 W	nd	nd	nd	124.30±1.21^{b}	463.11±15.78^{c}	nd	1.08±0.45^{a}	4.83±0.22^{a}	3.92±0.79^{a}	102.26±10.86^{d}	nd	nd	0.21±0.03^{b}
Simulated intestinal digested													
F	27.50±1.07^{a}	nd	nd	1225.20±43.03^{a}	3601.10±173.56^{b}	nd	nd	121.05±4.80^{a}	nd	4242.51±111.29^{a}	nd	nd	nd
C	2.22±0.13^{c}	nd	87.78±1.76^{a}	130.78±4.27^{c}	1528.21±165.85^{a}	47.98±0.83	nd	3.96±0.16^{c}	nd	277.29±11.99^{c}	nd	nd	nd
50 W	2.59±0.16^{bc}	nd	52.69±0.76^{b}	81.42±4.15^{d}	612.60±74.43^{b}	nd	nd	nd	nd	115.19±12.56d	nd	nd	nd
100 W	3.23±0.23^{b}	nd	32.32±1.03^{c}	72.00±4.17^{e}	546.48±60.41^{b}	nd	nd	4.30±0.20^{bc}	nd	359.61±35.20^{b}	nd	nd	nd
150 W	2.35±0.09^{bc}	nd	nd	142.10±3.17^{b}	590.84±18.73^{b}	nd	nd	4.72±0.12^{b}	nd	564.05±6.6	nd	nd	nd

F, sample of fresh mushroom; C, control sample dried at 40°C with HPD; 50 W, dried at 40°C with 50 W IR-HPD; 100 W, dried at 40°C with 100 W IR-HPD; 150 W, dried at 40°C with 150 W IR-HPD. 3,4DHBA, 3,4-Dihydroxybenzoic acid; 4HBA, 4-Hydroxybenzoic acid; nd, not detected. a,bValues followed by different lower letters within the same column are significantly different ($p<0.05$).

Table 7. Analytical parameters for liquid chromatography tandem-mass spectrometry analysis.

Phenolic compound	Calibration parameters					Mass spectrophotometer parameters						
						Ions for quantitative determination				Ions for qualitative determination		
	RT min	Calibration range (µg/L)	Regression equation	R^2	LOQ µg/kg	PI	1. TI	CE (V)	IR	PI	2. TI	CE (V)
Chrysophanol	13.161	1-50	y = (3,41408e+006)x + (3,45854e+006)	0.9986	0.04	254.2>	83.0	-18	51.3	254.2>	111.0	-17
Protocatechuic acid	1.991	1-100	y = (184712)x + (93768,7)	0.9960	3.14	152.9>	109.0	14	5.4	152.9>	90.9	26
Caffeic acid	2.670	1-100	y = (179908)x + (86789,5)	0.9968	2.37	178.8>	135.1	17	2.6	178.8>	89.2	33
o-Salicylic acid	5.064	1-100	y = (417587)x + (244556)	0.9960	0.68	137.1>	93.0	17	8.2	137.1>	65.0	29
p-Salicylic acid	2.603	1-100	y = (62659,0)x + (122404)	0.9969	1.62	137.0>	93.0	15	6.8	137.0>	65.1	29
Ellagic acid	3.406	1-100	y = (28492,2)x + (25479,3)	0.9956	0.23	301.0>	284.0	28	95.8	301.0>	300.0	29
Rutin	3.102	1-100	y = (257382)x + (390857)	0.9951	0.05	609.1>	300.0	37	37.0	609.1>	271.1	54
Hesperidin	3.913	1-100	y = (113302)x + (186818)	0.9958	0.27	609.0>	301.0	28	4.8	609.0>	303.1	27
Isoquercitrin	3.446	1-100	y = (249719)x + (407356)	0.9953	0.14	463.1>	300.0	27	55.6	463.1>	271.0	42
Vanillin	3.550	1-100	y = (18661,8)x + (34630,2)	0.9955	0.92	151.0>	136.1	17	38,9	151.0>	92.1	21
p-Coumaric acid	3.543	1-100	y = (108036)x + (267007)	0.9955	1.00	163.1>	119.1	16	0.2	163.1>	146.0	16
Luteolin	5.895	1-100	y = (298540)x + (546559)	0.9951	0.05	284.9>	133.1	34	15.9	284.9>	151.0	25
Quercetin	5.952	1-100	y = (218917)x + (626208)	0.9952	0.03	301.0>	151.2	22	63.1	301.0>	179.0	18

RT, retention time; LOQ, limit of quantification; PI, precursor ion (parent ion); TI, transition ion (daughter ion); CE, collision energy; IR, ion ratio.

(Çayan *et al.*, 2020; Wagay *et al.*, 2019). However, analyses of undigested *Agaricus bisporus* mushrooms did not yield the same result (Çayan *et al.*, 2020; Elhusseiny *et al.*, 2021). Food's phenolic components can be found higher after digestion than in the initial stage (Lafarga *et al.*, 2019). Cuvas-Limon *et al.,* who examined different phenolic compounds, reported that ellagic acid was observed in higher amounts after the digestion phases (Cuvas-Limon *et al.*, 2022). In addition, when we consider the effect of thermal treatment on the degradation of phenolic compounds (Kayacan *et al.*, 2020), it may be considered that the result we obtained in our study is compatible with the literature data.

P-salicylic, *p*-coumaric and protocatechuic acids were reported as the most abundant phenolic compounds in mushrooms by (Nowacka *et al*., 2014). Similar to our study, *p*-salicylic acid (25.59 mg/kg) was determined the most abundant phenolic acid form *Agaricus bisporus* by (Barros *et al*., 2009).

The distribution of individual phenolic contents was consistent with the TPC results. A significant decrease was observed in the amount of phenolic components of dried mushroom slices compared to the fresh sample. The contents of individual phenolics in mushroom slices were significantly reduced ($p<0.05$) after drying, except for protocatechuic acid, which increased by 31.30% at 100 W IR-HPD. *P*-salicylic acid was the least degraded phenolic, with a maximum decrease of 3.45 times after 150 W IR-HPD.

Moreover, when applying 100 W IR-HPD, there was no statistical change in *p*-salicylic acid ($p>0.05$). The degradation of phenolics after the drying process may be explained by irreversible chemical changes in phenolic compounds, which may occur due to long-term heat treatments (Zhou *et al*., 2017). Moreover, other factors such as the activity of oxidative enzymes (polyphenol oxidase, peroxidase), organic acid content, sugar concentration, and pH can also lead to phenolics deterioration. These results agree with Kayacan *et al*. (2020) who reported that the thermal treatments caused degradations in the phenolics.

Chrysophanol was not detected after *in vitro* simulated gastric digestion, whereas its content was higher after *in vitro* simulated intestinal digestion than an undigested fresh sample. The vanillin content was increased after *in vitro* simulated gastric (2.55 times) and intestinal (2.71 times) digestion compared to the fresh sample. The increase of phenolic compounds after digestion in the intestinal phase might be related to 2 more hours of extraction time and the effect of the enzymes (lipase, amylase and pancreatin or protease activity) in the food matrix, facilitating the release of the phenolic compounds bound to the matrix (Bouayed *et al*., 2011).

The protocatechuic acid content of fresh mushroom slices decreased by 90.63% after *in vitro* simulated gastric digestion, and it was not detected in dried samples after *in vitro* gastric and intestinal digestion. Similar results linked to bounding to the extracted matrix by ester or glycoside bounds also during digestion (Odriozola-Serrano *et al.*, 2023). Caffeic acid content decreased between 71.79 and 98.13% after drying, and while it was not detected after *in vitro* simulated gastric digestion, it was determined after *in vitro* intestinal digestion in amounts as low as 35.44 (°C), 85.67 (50 W) and 93.84 (100 W) % compared to undigested samples. IR-HPD drying at 100 W gave the highest results regarding protocatechuic acid and caffeic acid in all drying conditions. *O*-salicylic acid and *p*-salicylic acid values decreased between 60.67-86.29% and 71.13-94.60% after *in vitro* gastric digestion compared to undigested samples. After *in vitro* intestinal digestion simulation, variable results were obtained. For example, after simulated *in vitro* intestinal digestion, the amount of *o*-salicylic acid in fresh mushroom slices decreased by 14.37%, while *p*-salicylic acid increased by 41.57% compared to the values obtained in *in vitro* simulated gastric digestion. After drying, applying 150 W and 100 W IR-HPD caused minimum degradation of o-salicylic acid and p-salicylic acid. In a study performed on wild edible mushrooms (*Hericium erinaceus* and *Hericium coralloides*) detected degradation of *p*-salicylic acid with post-gastric and post-intestinal digestion (Heleno *et al.*, 2015a). Similarly, another study carried out by (Heleno *et al.*, 2015b), on two other wild mushroom species (*Volvopluteus gloiocephalus* and *Clitocybe subconnexa*) gave the same results both for *p*-salicylic and protocatechuic acid. The authors emphasised the possibility of linking phenolic compounds with other molecules, such as polysaccharides, that might make it difficult to cross the dialysis membrane. This fact can be considered for *o*-salicylic acid as well.

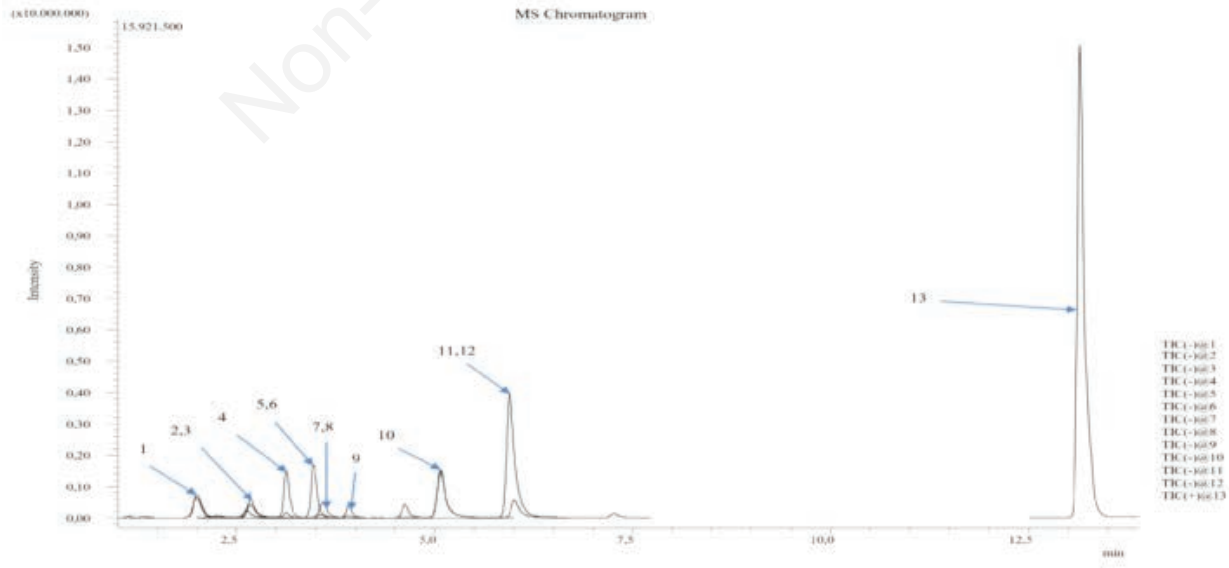

Figure 5. Liquid chromatography tandem-mass spectrometry chromatogram of the mushroom sample. 1, protocatechuic acid; 2, p-salicylic acid; 3, caffeic acid; 4, rutin; 5, ellagic acid; 6, isoquercitrin; 7, p-coumaric acid; 8, vanillin; 9, hesperidin; 10, o-salicylic acid; 11, luteolin; 12, quercetin; 13, chrysophanol.

Isoquercitrin, quercetin, and rutin contents completely disappeared after *in vitro* simulated gastric digestion (except for 100 and 150 W) and after *in vitro* intestinal digestion. Many vegetables, including mushrooms, contain significant amounts of dietary fibre. It has been suggested that dietary fibre has binding effects on some plant polyphenols and reduces bioaccessibility by limiting the diffusion of enzymes to their substrates (Palafox-Carlos *et al*., 2011). Therefore, the decrease in quercetin glycosides may be related to the presence of dietary fibres. Similarly, *p*-coumaric acid and luteolin contents completely disappeared after *in vitro* simulated gastric and intestinal digestions. Hesperidin content in dried mushroom slices was reduced after simulated intestinal digestion. Hesperidin in fresh mushroom samples was not detected after *in vitro* simulated gastric digestion, whereas a 73.97% reduction was observed after *in vitro* simulated intestinal digestion.

Colour values

The colour parameters acquired from the fresh and dried mushroom slices are presented in Table 8. *L** values indicated the lightness/darkness of mushroom slices, which were measured between 46.72 and 65.32. The fresh sample showed the highest *L** value so the brightest mushroom sample can be called fresh mushroom slices. When mushroom slices dried at 40°C HPD, *L** value was decreased. Kantrong *et al*. (2014) analysed colour parameters of microwave-vacuum dried (MVD) mushroom samples and MVD with IR-dried mushroom samples. They used 100 W and 200 W infrared radiation. In this study, the drying process led to a decrease in the *L** value and also the highest *L** value was obtained from a fresh sample. Colour parameters of mushrooms are important quality factors for both consumers and producers. Enzymatic and non-enzymatic reactions between carbohydrates, amino acids and reduced saccharides lead to the formation of brown compounds during the drying process. These compounds decrease *L** value, which is undesirable as it causes darkening in colour (Wang *et al*., 2014). The lowest *L** value was found in the dried sample by IR-HPD at 50 W. When IR power was increased to 100 W, the *L** value of the mushroom sample was the highest. IR drying can inactivate browning reactions; besides, some studies showed that increasing IR power provided faster inactivation of enzymatic browning reactions (Kantrong *et al*., 2014). *a** and *b** values of mushroom samples were measured between 2.35-6.31 and 18.80-30.54, respectively. *ΔE** value is an important factor indicating the total colour change. When the *ΔE** value is below 1.5 and above 6 can be interpreted as not visible and visible, respectively, for consumers (Kantrong *et al*., 2014). The *ΔE** values of dried mushrooms were found between 11.40 and 21.53 and fell into the clearly visible category.

There was no significant difference between C* and *h*° values of Control (C), and the samples dried at 50 W, 100 W, and 150 W IR-HPD except for fresh samples. Wang *et al*. (2014) dried shiitake mushroom slices using three different drying methods [mid-infrared assisted convection drying (MIRCD), hot air coupled with radio frequency drying and hot air coupled with microwave drying]. They measured the *a** and *b** values of fresh samples as 7.61 and 16.72, respectively. In addition, the *a** and *b** values of MIRCD mushroom samples were found to be 6.71 and 14.72, respectively. Similar to our study, *b** values which indicate blueness/yellowness, were determined to be higher than *a** values (greenness/redness). Also, when the MIRCD method was compared with the other two methods, they reported that the best colour parameters were obtained in the MIRCD method because of the inactivation of the browning reactions when using IR for drying. In another study that used freeze drying (FD) and hot air convective drying (CD), Leiva-Portilla *et al*. (2020) reported that *a** values of dried mushroom slices were measured as 12.04 (FD) and 14.38 (CD) and *b** values of samples were determined as 34.90 (FD) and 41.07 (CD).

Thermal camera images of mushroom slices

The thermal imaging camera has exclusive superiority in determining the surface temperature of materials because it can convert the invisible IR radiation generated by objects into visible thermal images (Su *et al*., 2020). The thermal camera images of IR (50, 100 and 150 W) assisted HPD and HPD without IR systems are given in Figure 6. The maximum temperatures of IR lamps at 50, 100 and 150 W were measured as 109.5, 118.9 and 122°C, respectively. Due to the geometric differences between the lamps, the temperatures are not the same at every point of the lamp. Regardless of the infrared lamp capacities, it was determined that the cabin temperature was uniform and averaged 40°C in all experiments. It was caused by the continuous variability of the interior air, whereas it has been observed that IR lamps were not effective in increasing the interior temperature of the cabinet.

The product temperatures of IR-HPD and without IR-dried mushrooms are given in Figure 7. Red, green and blue regions in the thermal images correspond to higher, medium and lower temperatures of mushroom slices during the dehydration period, respectively (Figure 7). While the temperatures of control samples have a homogeneous distribution in the drying process, it has been determined that IR-HPD dried mushrooms eliminate this homogeneous distribution. The cause is an unequal power distribution in the powerful IR field, which might cause local temperatures to be too high for even drying (Su *et al*., 2020). While the maximum temperature of the control sample was 35.4°C, the maximum temperatures of the products in the IR-HPD process dried at 50, 100, and 150 W were determined as 36.7, 41.3 and 41.5°C, respectively.

Table 8. Colour values of mushroom slices.

Sample	*L**	*a**	*b**	*△E**	*C**	*h*°
F	65.32±0.38^{a}	2.35±0.66^{b}	30.54±0.90a	-	30.64±0.86^{a}	85.58±1.36^{a}
C	56.48±0.51^{abc}	5.20±1.72^{a}	24.17±0.31b	11.40±5.19^{b}	24.78±0.29^{b}	77.64±0.46^{b}
50 W	46.76±1.95^{c}	6.31±0.87^{a}	20.06±0.23^{b}	21.53±3.31^{a}	21.06±0.21^{b}	72.38±0.33^{b}
100 W	64.12±1.26^{ab}	4.10±1.76^{ab}	18.80±0.36^{b}	15.93±2.08^{ab}	19.32±0.34^{b}	77.19±0.60^{b}
150 W	52.08±1.70^{bc}	4.53±0.28^{ab}	21.82±0.38^{b}	14.92±4.12^{ab}	22.29±0.37^{b}	78.14±0.13^{b}

F, sample of fresh mushroom; C, control sample dried at 40°C with HPD; 50 W, dried at 40°C with 50 W IR-HPD; 100 W, dried at 40°C with 100 W IR-HPD; 150 W, dried at 40°C with 150 W IR-HPD. Values followed by different lower letters within the same column are significantly different ($p<0.05$).

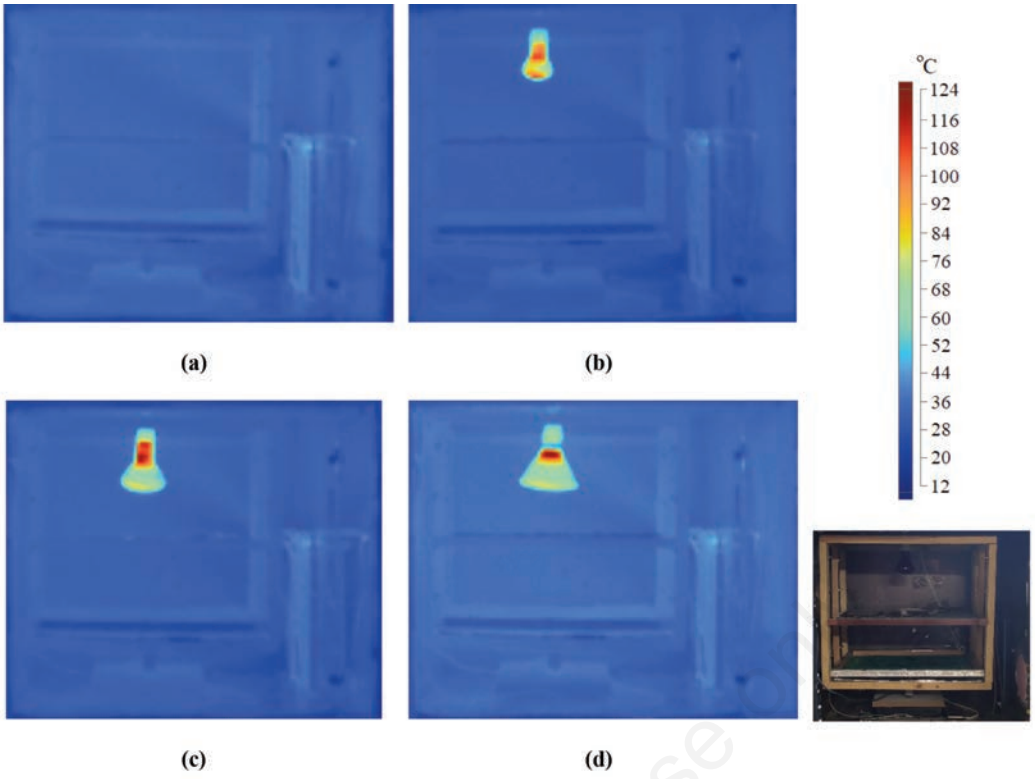

Figure 6. Thermal camera images of the drying system. **a)** Control sample dried at 40°C with heat pump drying; **b)** 50 W, dried at 40°C with 50 W infrared-assisted heat pump drying; **c)** 100 W, dried at 40°C with 100 W infrared-assisted heat pump drying; **d)** 150 W, dried at 40°C with 150 W infrared-assisted heat pump drying.

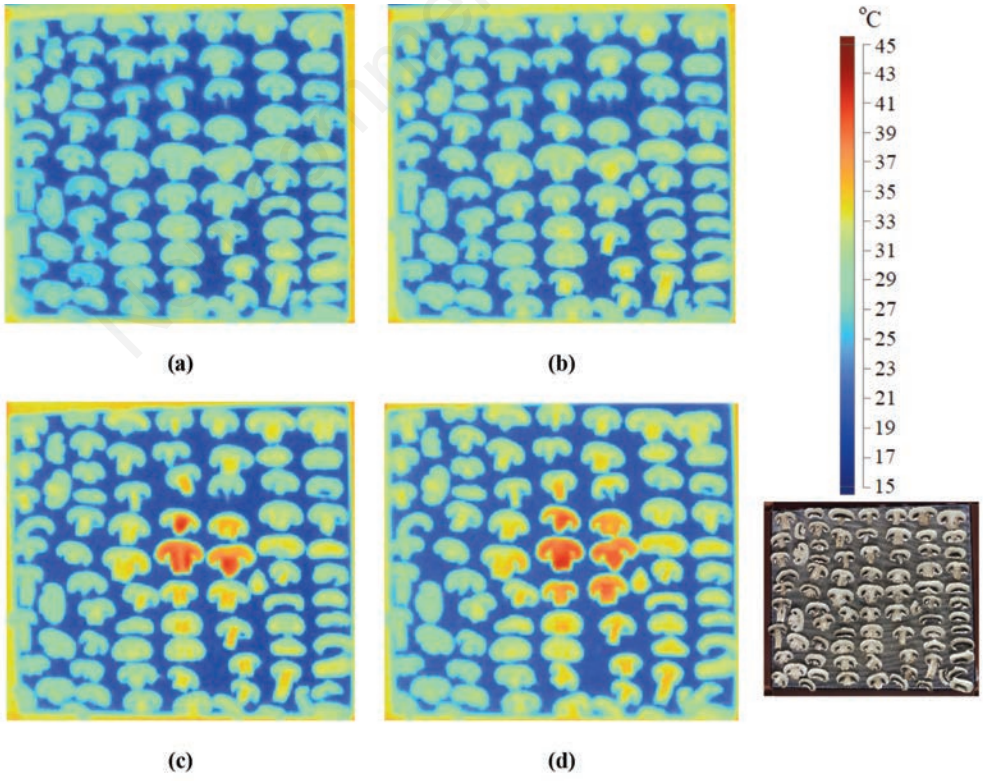

Figure 7. Thermal camera images of dried mushroom samples as removed from the dryer. **a)** Control sample dried at 40°C with heat pump dryin; **b)** 50 W, dried at 40°C with 50 W infrared-assisted heat pump drying; **c)** 100 W, dried at 40°C with 100 W infrared-assisted heat pump drying; **d)** 150 W, dried at 40°C with 150 W infrared-assisted heat pump drying.

In the 100 and 150 W IR-HPD drying systems, while the temperature inside the cabinet is kept constant at an average of 40°C, as in other drying conditions, it has been determined that IR lamps increase the temperature of the products in the middle regions close to the lamp by approximately 1.5°C. However, when a 50 W IR lamp is used, it has been observed that the temperature difference between the products near and far from the lamp is approximately 1°C. In addition, although the maximum temperatures are close to each other (41.3 and 41.5°C) when 100 and 150 W are applied, it has been determined by thermal camera images that using 150 W infrared lamps affects more products than 100 W.

Conclusions

The present study demonstrated the impacts of hybrid drying (IR-HPD) on drying characteristics, colour, thermal imaging and bioaccessibility of phenolics and AC of mushroom slices. The results showed that IR-HPD shortened the drying time between 33 and 93 min when compared with control (HPD), and its effect increased when IR power increased. Moreover, using IR for assisting HPD provided 13.11 to 30.77% less energy consumption than the control sample. The best models for predicting the drying kinetics of mushroom slices were the Page and Modified Page models. The D_{eff} values ranged from $9.023x10^{-10}$ m^2s^{-1}. In the IR-assisted samples, the D_{eff} value increased up to 39% compared to the control. TAC, AC and individual phenolics in mushroom slices decreased after drying compared with fresh samples. The increment in IR power caused the reduction in TPC and AC. 50 W IR power showed the highest TPC and AC while the highest individual phenolic contents were obtained from generally 100 W IR-HPD among dried samples. *In vitro* bioaccessibility of individual phenolic compounds and AC generally decreased. However, TPC values increased between 57 and 185% after *in vitro* simulated intestinal digestion compared to undigested samples. *L*, b*, C**, and *h*° values generally decreased while the *a** value determined that the lamps did not affect the interior temperature of the cabinet but increased after drying of mushroom slices. In HPD systems where IR lamps were used, it affected the product temperatures close to the lamp. This situation caused the products in the same tray to differ in drying times. Therefore, future studies should focus on obtaining the effects of the lamps on the drying time of the products more clearly by positioning the IR lamps at an equal distance from all the products in the cabinet. In addition, the distances of the IR lamps to the products should be examined and the optimum lamp distances where the products are dried homogeneously should be determined. Moreover, from the results obtained, IR-HPD can be a promising method because of its advantages. The findings of this comprehensive study are expected to guide manufacturers on the process design of the mushroom slices and the optimisation of the process parameters. Further studies may be by using IR lamps with different powers should be conducted in order to enlighten the contribution of IR-HPD to the drying kinetics and quality attributes of mushroom slices.

References

Abbaspour-Gilandeh Y., Kaveh M., Aziz M. 2020. Ultrasonic-Microwave and Infrared Assisted Convective Drying of Carrot: Drying Kinetic, Quality and Energy Consumption. Appl. Sci. 10.

Adak N., Heybeli N., Ertekin C. 2017. Infrared drying of strawberry. Food Chem. 219:109-116.

Ali M.M., Hashim N., Aziz S. A., Lasekan O. 2020. Emerging non-destructive thermal imaging technique coupled with chemometrics on quality and safety inspection in food and agriculture. Trends Food Sci. Technol. 105:176-85.

Barros L., Dueñas M., Ferreira I.C.F.R., Baptista P., Santos-Buelga C. 2009. Phenolic acids determination by HPLC–DAD–ESI/MS in sixteen different Portuguese wild mushrooms species. Food Chem. Toxicol. 47:1076-9.

Benzie I.F.F., Strain J.J. 1996. The Ferric Reducing Ability of Plasma (FRAP) as a Measure of "Antioxidant Power": The FRAP Assay. Anal. Biochem. 239:70-6.

Bouayed J., Hoffmann L., Bohn T. 2011. Total phenolics, flavonoids, anthocyanins and antioxidant activity following simulated gastrointestinal digestion and dialysis of apple varieties: Bioaccessibility and potential uptake. Food Chem. 128:14-21.

Cao X.H., Zhang M., Qian H., Mujumdar A.S. 2017. Drying based on temperature-detection-assisted control in microwave-assisted pulse-spouted vacuum drying. J. Sci. Food Agric. 97:2307-15.

Coşkun S., Doymaz İ., Tunçkal C., Erdoğan S. 2017. Investigation of drying kinetics of tomato slices dried by using a closed loop heat pump dryer. Heat Mass Transf. 53:1863-71.

Crank J. 1975. The mathematics of diffusion (2nd ed). Clarendon Press.

Cuvas-Limon R.B., Ferreira-Santos P., Cruz M., Teixeira J.A., Belmares R., Nobre C. 2022. Effect of Gastrointestinal Digestion on the Bioaccessibility of Phenolic Compounds and Antioxidant Activity of Fermented Aloe vera Juices. Antioxidants. 11:2479.

Çayan F., Deveci E., Tel-Çayan G., Duru M. E. 2020. Identification and quantification of phenolic acid compounds of twenty-six mushrooms by HPLC-DAD. J. Food Meas. Charact. 14:1690-8.

Das I., Das S.K., Bal S. 2009. Drying kinetics of high moisture paddy undergoing vibration-assisted infrared (IR) drying. J. Food Eng. 95:166-71.

Delfiya D.S.A., Prashob K., Murali S., Alfiya P.V., Samuel M.P., Pandiselvam R. 2022. Drying kinetics of food materials in infrared radiation drying: A review. J. Food Process Eng. 45:e13810.

Deng Y., Wang Y., Yue J., Liu Z., Zheng Y., Qian B., Zhong Y., Zhao Y. 2014. Thermal behavior, microstructure and protein quality of squid fillets dried by far-infrared assisted heat pump drying. Food Control. 36:102-10.

Doymaz I. 2023. Influence of Infrared Drying on Some Quality Properties of Nashi Pear (Pyrus pyrifolia) Slices. Erwerbs-Obstbau, 65:47-54.

Doymaz İ. 2014. Infrared drying of button mushroom slices. Food Sci. Biotechnol. 23:723-9.

Elhusseiny S.M., El-Mahdy T.S., Awad M.F., Elleboudy N.S., Farag M.M., Aboshanab K.M., Yassien M.A. 2021. Antiviral, cytotoxic, and antioxidant activities of three edible agaricomycetes mushrooms: Pleurotus columbinus, Pleurotus sajor-caju, and Agaricus bisporus. J. Fungi. 7:645.

Gasecka M., Siwulski M., Mleczek M. 2018a. Evaluation of bioactive compounds content and antioxidant properties of soil-growing and wood-growing edible mushrooms. J. Food Process. Pres. 42:e13386.

Gasecka M., Magdziak, Z., Siwulski M., Mleczek M. 2018b. Profle of phenolic and organic acids, antioxidant properties

and ergosterol content in cultivated and wild growing species of Agaricus. Eur. Food Res. Technol. 244:259-68.
Geng Z.H., Torki M., Kaveh M., Beigi M., Yang X.H. 2022. Characteristics and multi-objective soptimisation of carrot dehydration in a hybrid infrared/hot air dryer. Lwt-Food Sci. Technol. 172:114229.
Ghanbarian D., Dastjerdi M.B., Torki-Harchegani M. 2016. Mass transfer characteristics of bisporus mushroom (*Agaricus bisporus*) slices during convective hot air drying. Heat Mass Transf. 52:1081-8.
Gopirajah R., Choudhary A., Anandharamakrishnan C. 2018. Computational modeling of dehydration of mushroom. MOJ Food Process. Technol. 6:264-70.
Gursoy N., Sarikurkcu C., Cengiz M., Solak M.H. 2009. Antioxidant activities, metal contents, total phenolics and flavonoids of seven Morchella species. Food Chem. Toxicol. 47:2381-8.
Heleno S.A., Barros L., Martins A., Morales P., Fernandez-Ruiz V., Glamoclija J., Ferreira I. C. 2015b. Nutritional value, bioactive compounds, antimicrobial activity and bioaccessibility studies with wild edible mushrooms. LWT-Food Sci. Technol. 63:799-806.
Heleno S.A., Barros L., Martins A., Queiroz M.J.R., Morales P., Fernández-Ruiz V., Ferreira I.C. 2015a. Chemical composition, antioxidant activity and bioaccessibility studies in phenolic extracts of two Hericium wild edible species. LWT-Food Sci. Technol. 63:475-81.
Islam T., Yu X., Xu B. 2016. Phenolic profiles, antioxidant capacities and metal chelating ability of edible mushrooms commonly consumed in China. LWT - Food Sci. Technol. 72:423-31.
Jaworska G., Pogoń K., Bernaś E., Duda-Chodak A. 2015. Nutraceuticals and Antioxidant Activity of Prepared for Consumption Commercial Mushrooms Agaricus bisporus and Pleurotus ostreatus. J. Food Qual. 38:111-22.
Kamiloglu S., Capanoglu E. 2014. In vitro gastrointestinal digestion of polyphenols from different molasses (pekmez) and leather (pestil) varieties. Int. J. Food Sci. Technol. 49:1027-39.
Kantrong H., Tansakul A., Mittal G.S. 2014. Drying characteristics and quality of shiitake mushroom undergoing microwave-vacuum drying and microwave-vacuum combined with infrared drying. J. Food Sci. Technol. 51:3594-608.
Kayacan S., Karasu S., Akman P.K., Goktas H., Doymaz I., Sagdic O. 2020. Effect of different drying methods on total bioactive compounds, phenolic profile, in vitro bioaccessibility of phenolic and HMF formation of persimmon. LWT. 118:108830.
Khampakool A., Soisungwan S., Park S.H. 2019. Potential application of infrared assisted freeze drying (IRAFD) for banana snacks: Drying kinetics, energy consumption, and texture. LWT. 99:355-63.
Kumaran A., Joel Karunakaran R. 2006. Antioxidant and free radical scavenging activity of an aqueous extract of Coleus aromaticus. Food Chem. 97:109-14.
Lafarga T., Villaró S., Bobo G., Simó J., Aguiló□Aguayo I. 2019. Bioaccessibility and antioxidant activity of phenolic compounds in cooked pulses. Int. J. Food Sci. Technol. 54:1816-23.
Leiva-Portilla D.J., Rodríguez-Núñez K.E., Rodríguez-Ramos F.J., Delgadillo Acevedo Á., Uribe, E. 2020. Impact on Physicochemical Composition and Antioxidant Activity of the Wild Edible Mushroom Cyttaria espinosae Subjected to Drying. Chem. Biodiver. 17:e2000642.
Li X., Li J., Wang R., Rahaman A., Zeng X.-A., Brennan C.S. 2021. Combined effects of pulsed electric field and ultrasound pretreatments on mass transfer and quality of mushrooms. LWT. 150:112008.
Liu Z.B., Zhang M., Wang Y.C. 2016. Drying of restructured chips made from the old stalks of Asparagus officinalis: impact of different drying methods. J. Sci. Food Agric. 96:2815-24.
Lombrana J.I., Rodriguez R., Ruiz U. 2010. Microwave-drying of sliced mushroom. Analysis of temperature control and pressure. Innov. Food Sci. Emerg. Technol. 11:652-60.
Minekus M., Alminger M., Alvito P., Ballance S., Bohn T., Bourlieu C., … & Brodkorb A. 2014. A standardised static in vitro digestion method suitable for food – an international consensus. Food & Funct. 5:1113-24.
Mirzaei-Baktash H., Hamdami N., Torabi P., Fallah-Joshaqani S., Dalvi-Isfahan M. 2022. Impact of different pretreatments on drying kinetics and quality of button mushroom slices dried by hot-air or electrohydrodynamic drying. LWT. 155:112894.
Naknaen P., Itthisoponkul T., Charoenthaikij P. 2015. Proximate compositions, nonvolatile taste components and antioxidant capacities of some dried edible mushrooms collected from Thailand. J Food Meas. Charact. 9:259-68.
Nowacka N., Nowak R., Drozd M., Olech M., Los R., Malm A. 2014. Analysis of phenolic constituents, antiradical and antimicrobial activity of edible mushrooms growing wild in Poland. LWT - Food Sci. Technol. 59:689-94.
Nowacka N., Nowak R., Drozd M., Olech M., Los R., Malm A. 2015. Antibacterial, Antiradical Potential and Phenolic Compounds of Thirty-One Polish Mushrooms. PLOS ONE. 10:e0140355.
Odriozola-Serrano I., Nogueira D.P., Esparza I., Vaz A.A., Jiménez-Moreno N., Martín-Belloso O., Ancín-Azpilicueta C. 2023. Stability and Bioaccessibility of Phenolic Compounds in Rosehip Extracts during In Vitro Digestion. Antioxidants. 12:1035.
Palacios I., Lozano M., Moro C., D'arrigo M., Rostagno M.A., Martínez J.A., Villares A. 2011. Antioxidant properties of phenolic compounds occurring in edible mushrooms. Food Chem. 128:674-8.
Palafox-Carlos H., Ayala-Zavala J.F., González-Aguilar G.A. 2011. The Role of Dietary Fiber in the Bioaccessibility and Bioavailability of Fruit and Vegetable Antioxidants. J. Food Sci. 76:R6-R15.
Peter M.C., Liu Z.W., Fang Y.L., Dou X.L., Awuah E., Soomro S.A., Chen K.J. 2021. Computational intelligence and mathematical modelling in chanterelle mushrooms' drying process under heat pump dryer. Biosyst. Eng. 212:143-59.
Piskov S., Timchenko L., Grimm W.D., Rzhepakovsky I., Avanesyan S., Sizonenko M., Kurchenko V. 2020. Effects of Various Drying Methods on Some Physico-Chemical Properties and the Antioxidant Profile and ACE Inhibition Activity of Oyster Mushrooms (Pleurotus Ostreatus). Foods. 9:160.
Rodriguez-Roque M.J., Rojas-Grau M.A., Elez-Martinez P., Martin-Belloso O. 2013. Soymilk phenolic compounds, isoflavones and antioxidant activity as affected by in vitro gastrointestinal digestion. Food Chem. 136:206-12.
Sadeghi E., Haghighi Asl A., Movagharnejad K. 2020. sOptimisation and quality evaluation of infrared-dried kiwifruit slices. Food Sci. Nutr. 8:720-34.
Sevik S., Aktas M., Dogan H., Kocak S. 2013. Mushroom drying with solar assisted heat pump system. Energy Convers. Manag. 72:171-8.
Shi J., Pan Z., McHugh T.H., Wood D., Hirschberg E., Olson D. 2008. Drying and quality characteristics of fresh and sugar-

infused blueberries dried with infrared radiation heating. LWT - Food Sci. Technol. 41:1962-72.

Su D.B., Lv W.Q., Wang Y., Li D., Wang L.J. 2020. Drying characteristics and water dynamics during microwave hot-air flow rolling drying of Pleurotus eryngii. Dry. Technol. 38:1493-504.

Sufer O., Palazoglu T.K. 2019. A study on hot-air drying of pomegranate Kinetics of dehydration, rehydration and effects on bioactive compounds. J. Therm. Anal. Calorim. 137:1981-90.

Taskin H., Sufer O., Attar S.H., Bozok F., Baktemur G., Buyukalaca S., Kafkas N.E. 2021. Total phenolics, antioxidant activities and fatty acid profiles of sixMorchellaspecies. J. Food Sci. Technol. Mysore, 58:692-700.

Tirawanichakul S., Phatthalung W.N., Tirawanichakul Y. 2008. Drying Strategy of Shrimp using Hot Air Convection and Hybrid Infrared Radiation/Hot Air Convection. Walailak J. Sci. Technol. (WJST). 5:1.

Topuz F.C., Bakkalbasi E., Aldemir A., Javidipour I. 2022. Drying kinetics and quality properties of Mellaki (Pyrus communis L.) pear slices dried in a novel vacuum-combined infrared oven. J. Food Process. Preserv. 46:e16866.

Tunckal C., Ozkan-Karabacak A., Tamer C.E., Yolci-Omeroglu P., Goksel Z. 2022. Mathematical Modelling And Optimisation Of Melon Slice Drying With Response Surface Methodology In A Heat Pump Drying System. Lat. Ame Appl. Res. 52:101-10.

Ucar T.M., Karadag A. 2019. The effects of vacuum and freeze-drying on the physicochemical properties and in vitro digestibility of phenolics in oyster mushroom (Pleurotus ostreatus). J. Food Meas. Charact. 13:2298-309.

Velioglu Y.S., Mazza G., Gao L., Oomah B.D. 1998. Antioxidant Activity and Total Phenolics in Selected Fruits, Vegetables, and Grain Products. J. Agric. Food Chem. 46:4113-7.

Vishwanathan K.H., Giwari G.K., Hebbar H.U. 2013. Infrared assisted dry-blanching and hybrid drying of carrot. Food Bioprod. Process. 91:89-94.

Vu D.C., Vo P.H., Coggeshall M.V., Lin C.-H. 2018. Identification and sCharacterisation of Phenolic Compounds in Black Walnut Kernels. J. Agric. Food Chem. 66:4503-11.

Wagay J.A., Nayik G.A., Wani S.A., Mir R.A., Ahmad M.A., Rahman Q.I., Vyas D. 2019. Phenolic profiling and antioxidant capacity of Morchella esculenta L. by chemical and electrochemical methods at multiwall carbon nanotube paste electrode. J. Food Meas. Charact. 13:1805-19.

Wang X., Yu J., Zhou M., Lv X. 2014. Comparative studies of ejector-expansion vapor compression refrigeration cycles for applications in domestic refrigerator-freezers. Energy. 70:635-42.

Xu B., Wang D.Y., Li Z.H., Chen Z.Q. 2021. Drying and dynamic performance of well-adapted solar assisted heat pump drying system. Renew. Energy. 164:1290-305.

Zeng X., Suwandi J., Fuller J., Doronila A., Ng K. 2012. Antioxidant capacity and mineral contents of edible wild Australian mushrooms. Food Sci. Technol. Int. 18:367-79.

Zhang L., Jiang L., Xu Z., Zhang X., Fan Y., Adnouni M., Zhang C. 2022. sOptimisation of a variable-temperature heat pump drying process of shiitake mushrooms using response surface methodology. Renew. Energy, 198:1267-78.

Zhou L.Y., Cao Z.Z., Bi J.F., Yi J.Y., Chen Q.Q., Wu X.Y., Zhou M. 2016. Degradation kinetics of total phenolic compounds, capsaicinoids and antioxidant activity in red pepper during hot air and infrared drying process. Int. J. Food Sci. Technol. 51:842-53.

Zhou L., Guo X., Bi J., Yi J., Chen Q., Wu X., Zhou M. 2017. Drying of Garlic Slices (Allium Sativum L.) and its Effect on Thiosulfinates, Total Phenolic Compounds and Antioxidant Activity During Infrared Drying. J. Food Process. Preserv. 41:e12734.